



Electrochemical application of ZnCr₂O₄@MWCNTs-modified carbon paste electrode for sensing of chlorthalidone in its biological fluids

Ahmed M. Abdel-Raouf¹ · Manal M. Fouad^{1,2} · Noha S. Rashed¹ · Asmaa I. Hosameldin¹ · Elsayed Elgazzar³

Received: 13 December 2022 / Accepted: 13 June 2023 / Published online: 14 July 2023
© Iranian Chemical Society 2023

Abstract

A new method for chlorthalidone (CLT) determination was developed on multiwalled carbon nanotube-modified nanocrystalline zinc chromite carbon paste electrodes (ZnCr₂O₄@MWCNTs/CPEs). Electrochemical performance of CLT was assessed by a cyclic voltammetry (CV) and differential pulse voltammetry (DPV). The nanostructures ZnO, ZnCr₂O₄, and ZnCr₂O₄/MWCNTs were prepared by chemical co-precipitation method. The microstructural, composition, and mean size of the particles were identified using XRD, EDX, and TEM techniques. ZnO showed a well crystallinity of crystal size 32 nm, while the spinel ZnCr₂O₄ exhibited a small particle size of approximately 10 nm. ZnCr₂O₄/MWCNTs showed poor crystal structure affected by CNTs replacement. The EDX spectra affirm the presence of the elements Zn, Cr, O, and C into the nanocomposite lattice, and the TEM micrographs indicated the particles in hexagonal and spherical shapes with a small size. The modified electrode exhibited improved activity and great conductivity in comparison with the bare sensor without modification. The method was linear from 0.1–9 μmol L⁻¹ with a minimum detection limit of 0.03 μmol L⁻¹. Lastly, the proposed procedure was effectively accurate and selective for the determination of CLT in tablet and biological fluids. This novel sensor was considered as environmentally friendly assisted by Eco-scale approach.

Keywords Chlorthalidone · Spinel-structured ZnCr₂O₄ · Multiwalled carbon nanotubes · Green assessment · Differential pulse voltammetry

Introduction

In recent years, the use of electrochemical methods was considered as an alternative in the detection and analysis of food [1] and drugs [2–5] due to its wide range of applications, ease of use, wide variety of electrodes, and speedy readout. They can be used to measure trace levels of substances [6] and for the determination of exosomes from certain diseases [7]. They also offer excellent sensitivity and specificity and

provide fast, reliable, and early detection of cancer metastasis [8].

Moreover, nanoparticles inclusion to electrodes has significant advantages such as enhancing active surface area, mass transport, long-term stability, multiple functionalization, amplification of signals, and catalytic activity [1, 9, 10]. Cr/ZnO is an example of these nanoparticles having a variety of applications, including the photolytic degradation of aniline and the removal of nitrogen oxide pollutants. Different techniques have been utilized to fabricate ZnO and ZnCr₂O₄ including electrochemical deposition, hydrothermal, chemical vapor deposition, sol–gel, and co-precipitation approach [11, 12].

A literature survey revealed that there is no electrochemical method for determining CLT. In this work, scalable and cost-effective chemical co-precipitation method was utilized to prepare ZnCr₂O₄/MWCNTs which has been prepared and characterized. The objective of the present study is to develop a convenient and sensitive method for the determination of CLT based on the fabricated and characterized modified electrode in its dosage form, plasma and urine

✉ Asmaa I. Hosameldin
drasma13687@yahoo.com;
asmaahosameldin944.el@azhar.edu.eg

¹ Pharmaceutical Analytical Chemistry Department, Faculty of Pharmacy, Al-Azhar University, Nasr City, Cairo 11651, Egypt

² Pharmaceutical Analytical Chemistry Department, Faculty of Pharmacy, October University for Modern Sciences and Arts (MSA), Giza 11787, Egypt

³ Department of Physics, Faculty of Science, Suez Canal University, Ismailia, Egypt

samples. Electrochemical performance of the drug was assessed by CV and DPV. Finally, the produced method was assessed as an environmental ecofriendly technique.

CLT (Figure 1S) is white or yellowish-white crystalline powder. It is practically insoluble in water, chloroform, and ether and soluble in methyl alcohol [13]. CLT is an orally administered thiazide-like diuretic used to control hypertension and edema, including that concomitant with heart failure [14]. Numerous analytical methods have been established for the estimation of CLT including spectrophotometric [15–18], spectrofluorimetric [19], HPLC [20–25], chemometrics [25], TLC [26, 27], capillary zone electrophoresis [28], LC–MS–MS [29, 30], ultrafast liquid chromatography [31], and supercritical fluid chromatography methods [32].

Experimental

Instruments

Voltammetric assay was done using Bio-logic SP 150 electrochemical workstation attached to a specialized computer. The fabricated sensors were CPE, ZnO/CPE, ZnCr₂O₄/CPE, or ZnCr₂O₄/MWCNTs /CPE. X-ray diffractometer (XRD; Rigaku Smart Lab.) was employed to investigate the microstructure properties of the fabricated samples through 2θ changed between 20° and 80°. The elemental chemical composition and purity of ZnO, spinel ZnCr₂O₄, and ZnCr₂O₄/CNTs were characterized by energy-dispersive X-ray analysis (EDX; JEOL-JSM-7600F). Sputter coater (Model, EMS 150 T ES) was used to coat the nanopowder by iridium. To define the mean size and particle distribution, transmission electron microscopy (TEM; Hitachi-H-7500, Japan) was performed at 80 kV. Further, pH meter Jenway, UK 3510, and sonicator (cleanwise®) model WUC-A06H (Korea) were used during the preparation of the samples.

Materials and reagents

CLT pure sample was kindly provided by Egyptian Co for Pharmaceutical and Chemical Industries (10th of Ramadan City), Cairo, Egypt. The purity was (99.00 ± 0.21) as referred by the supplier. Hygroton® containing 50 mg CLT was purchased from local market. Methanol, highly pure graphite powder (10–20 μm), paraffin oil, Zn (CH₃COO)₂·2H₂O, and Cr (NO₃)₂·4H₂O were purchased from Sigma-Aldrich, Germany. Dipotassium hydrogen phosphate (K₂HPO₄), dihydrogen potassium phosphate (KH₂PO₄), orthophosphoric acid, and sodium hydroxide were purchased from El-Nasr Company, Egypt. Phosphate buffer solution (0.1 mol L⁻¹) composed of a mixture of 1 mol L⁻¹ K₂HPO₄ and 1 mol L⁻¹ KH₂PO₄; pH was adjusted using 0.1 mol L⁻¹ H₃PO₄ and 0.1 mol L⁻¹ NaOH.

Standard solution

Stock solution of CLT (1 × 10⁻³ mol L⁻¹) was prepared by dissolving 33.87 mg of CLT in 70 mL of methanol and shaken for 15 min, and then volume was completed to 100 mL with methanol.

Preparation of ZnO, ZnCr₂O₄ and ZnCr₂O₄/MWCNTs nanoparticles

Un-doped ZnO was prepared via chemical precipitation approach at room temperature. Firstly, to 65 mL 1 M aqueous solution zinc acetate dihydrate (Zn (CH₃COO)₂·2H₂O), 65 mL of 2 M sodium hydroxide (NaOH) was added dropwise under vigorous stirring. At pH ~ 10, a clear white precipitate of zinc hydroxide (Zn (OH)₂) was obtained. After completion of the reaction, the obtained white solid precipitate was filtered and washed with deionized water, dried at 70 °C for 12 h, and finally annealed in a furnace at 400 °C for 3 h. On the other side, the spinel compound ZnCr₂O₄ was prepared by dissolving 0.2 mol zinc acetate and 0.3 mol chromium nitrate Cr(NO₃)₂·4H₂O into 50 mL and 70 mL deionized water, respectively. Thereafter, 80 mL NaOH solution was carefully added till gray white powder was obtained at approximately pH 9. The formed powder was filtered, washed, dried, and calcined at the same previous procedures. The nanocomposite ZnCr₂O₄/MWCNTs was prepared by dissolving 0.05 g ZnCr₂O₄ into 15 mL MWCNTs (0.05 g MWCNTs into 50 mL deionized water). After that, the solution was heat-treated in a microwave oven. The resulting precipitate was centrifuged, washed many times, and left for drying [33].

Electrode fabrication

Carbon bare electrode was constructed by mixing 0.4 g graphite powder and 0.2 mL paraffin oil using a pestle and mortar. The formed homogenous paste was filled into the cavity of the sensor, and the surface was smoothed out to obtain a glossy appearance. Modified electrodes ZnO, ZnCr₂O₄, and ZnCr₂O₄/MWCNTs were fabricated by adding nanoparticles in a the ratio of 6–12% to 0.6 g graphite powder and 0.4 mL paraffin oil to create a uniform paste. All prepared sensors were constructed in a similar way as previously stated.

Electrochemical procedure

The voltammetric cell was filled with 25 mL of phosphate buffer of pH 5.0; then a suitable volume of CLT standard solution was used to get a concentration of 1×10^{-4} mol L⁻¹. All prepared electrodes were subjected to a definite voltage for a specified time. After the stated time, the potential and stirring were on hold for 6.0 s. All samples were determined in the same condition. Finally, differential pulse voltammograms were determined at the optimum state in DPV in a range 0.1–9 μ mol L⁻¹ with a scan rate of 100 mV/s, pulse amplitude of 20 mV, equilibrium time of 5 s, and a step potential of 5 mV.

Application to dosage form

Twenty Hygroton® tablets containing 50 mg CLT were accurately weighed and finely ground, and an amount of the fine powder equivalent to one tablet was transferred into a 100-mL volumetric flask, to which 60 mL methanol was added. After vigorously shaking for ten minutes, the flask was sonicated for 15 min, completed to the final volume with the same solvent, and then filtered. Further dilutions with phosphate buffer (pH 5) were done to prepare different concentrations of CLT; then the obtained solution was centrifuged at 5000 rpm for 15 min. The general procedure was repeated using aliquots covering the working concentration range, and the concentrations of CLT were calculated using the regression equation.

Spiked human plasma

Human plasma samples obtained from healthy individuals immediately prior to analysis were diluted five times using phosphate buffer (pH 5) to minimize the matrix effects prior to analysis. The samples were then spiked with suitable different concentrations of the drug (0.3–9 μ mol L⁻¹). CLT concentrations were determined in the plasma by the proposed method using the regression equation, and the recovery percent (%R) was determined.

Spiked human urine

A drug-free urine sample was provided by healthy non-smoking volunteer. The urine samples were spiked with suitable concentrations of CLT then centrifuged at 5000 rpm for 10 min to reduce the effect of any unexpected endogenous materials. The clear supernatant was diluted with phosphate buffer (pH 5) spiked with suitable concentrations of CLT (0.3–9 μ mol L⁻¹) and then completed to volume with the buffer. CLT was determined in the urine as mentioned above, and the drug concentrations were calculated from the corresponding regression equation.

Results and discussion

Characterization of ZnO, ZnCr₂O₄, and ZnCr₂O₄/MWCNTs nanocomposites

XRD, EDX, and TEM spectroscopy were used to explore the structural, chemical composition, and mean particle size of the nanoparticles ZnO, ZnCr₂O₄, and ZnCr₂O₄/MWCNTs. As can be seen from the XRD pattern in Fig. 1, ZnO has a polycrystalline structure of sharp, narrow, and high-intensity peaks suggesting a large crystallite size and well crystal structure. The diffraction peaks located at $2\theta = 32.27^\circ$, 34.85° , 36.67° , 47.95° , 56.93° , 63.30° , 66.83° , 68.29° , 69.61° , 72.97° , and 77.37° according to the typical reflection planes (100), (002), (101), (102), (110), (103), (200), (112), (201), and (004) coincide with the standard card of wurtzite hexagonal structure ZnO (JCPDS. 79–2205, space group P63mc). No other phases related to hydroxyl species or chemical salts existed in the spectrum [34, 35]. Besides, the nanostructures ZnCr₂O₄ exhibited wide peaks attributed to the small crystalline size. The characteristic diffraction peaks located at 30.30° , 35.73° , 43.31° , 54.07° , 57.47° , 62.83° , and 74.69° refer to the (220), (311), (400), (422), (511), (440), and (533) planes are indexed to the spinel cubic phase of zinc chromium oxide (ZnCr₂O₄, JCPDS 87-0028, space group Fd-3 m) [36, 37]. Although with the closeness of ionic radius of Zn²⁺ (0.074 nm) to Cr³⁺ (0.063 nm) and electronegativity of Zn (1.65) compared with Cr (1.66), the phase was modified to the spinel structure due to the high amount of Cr³⁺ replacements. Additionally, the nanocomposite ZnCr₂O₄/MWCNTs showed deterioration structure in which most of the peaks of the spinel compound disappeared by MWCNTs inclusion. Only the weak reflection peaks of the planes (311) and (440) were observed in the spectrum. Moreover, a broad peak associated with the (002) plane of graphitic structure was detected at approximately 26.60° . It

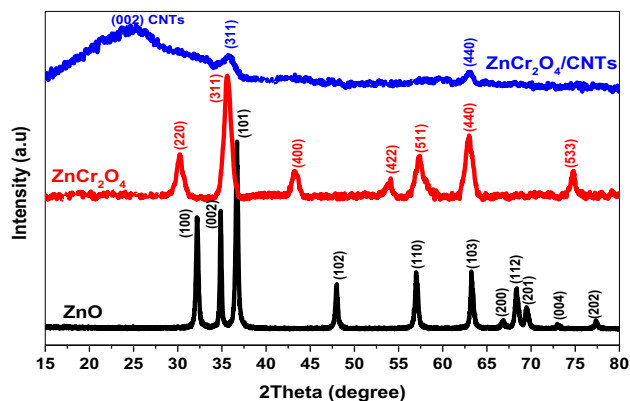


Fig. 1 XRD patterns of ZnO, ZnCr₂O₄, and ZnCr₂O₄/MWCNTs

is worthy to note that the low degree of crystallinity was due to the lower calcination temperature as well as the combination of amorphous structure (MWCNTs) and crystalline phase of ZnCr_2O_4 [38, 39].

To affirm the microstructure of the nanoparticles, the crystallographic parameters including the crystallite size (D), the dislocation density (δ), the degree of crystallinity (X_c), and the lattice strain (ε) were evaluated using the following equations [40–42]:

$$D = k\lambda/\beta \cos \theta \quad (1)$$

$$\delta = 1/D^2 \quad (2)$$

$$X_c = \beta/0.24 \quad (3)$$

$$\varepsilon = \beta/(4 \tan \theta) \quad (4)$$

Equation 1 represents Debye–Scherrer formula where λ is the wavelength of the incident X-ray radiation, K is the Scherrer's constant (the shape factor) ~ 0.94 , θ is the angle of the diffracted X-ray radiations (Bragg angle), D is the average crystallite size, and β is the width at half maximum (FWHM) recorded in radian. The obtained XRD data are presented in Table 1. As summarized in the table, ZnO demonstrated a big crystallite size compared to the spinel ZnCr_2O_4 which suddenly decreased to around 10 nm. The impact of size confinement is very useful in most of biological and electrochemical applications in which the surface area was significantly increased. Moreover, the degree of crystallinity was decreased, whereas the strain and dislocation density were increased due to the increase of Cr^{3+} ion defects.

The elemental composition of the prepared samples was recorded using EDX spectra. Figure 2a illustrates the EDX pattern of ZnO including zinc (Zn) and oxygen (O) elements. However, the spectrum of spinel ZnCr_2O_4 (Fig. 2b) revealed the presence of chromium ions which clearly assure the surface modification and again confirm the grown spinel ZnCr_2O_4 with no further peaks related to other elements. Figure 2c shows the EDX spectrum of $\text{ZnCr}_2\text{O}_4/\text{MWCNTs}$ composed of the elements Zn, O, Cr, and C [43]. The strong carbon peak detected in the spectrum displayed that the MWCNTs completely covered the spinel lattice which is

Table 1 The crystallographic parameters of the nanostructures ZnO, ZnCr_2O_4 , and $\text{ZnCr}_2\text{O}_4/\text{MWCNTs}$

The nanoparticles	D (nm)	$\delta \times 10^{-4} \text{ nm}^{-2}$	X_c	$\varepsilon \times 10^{-3}$
ZnO	32.00	9.80	47.41	4.02
$\text{ZnCr}_2\text{O}_4/\text{MWCNTs}$	10.00	100.00	15.66	11.70

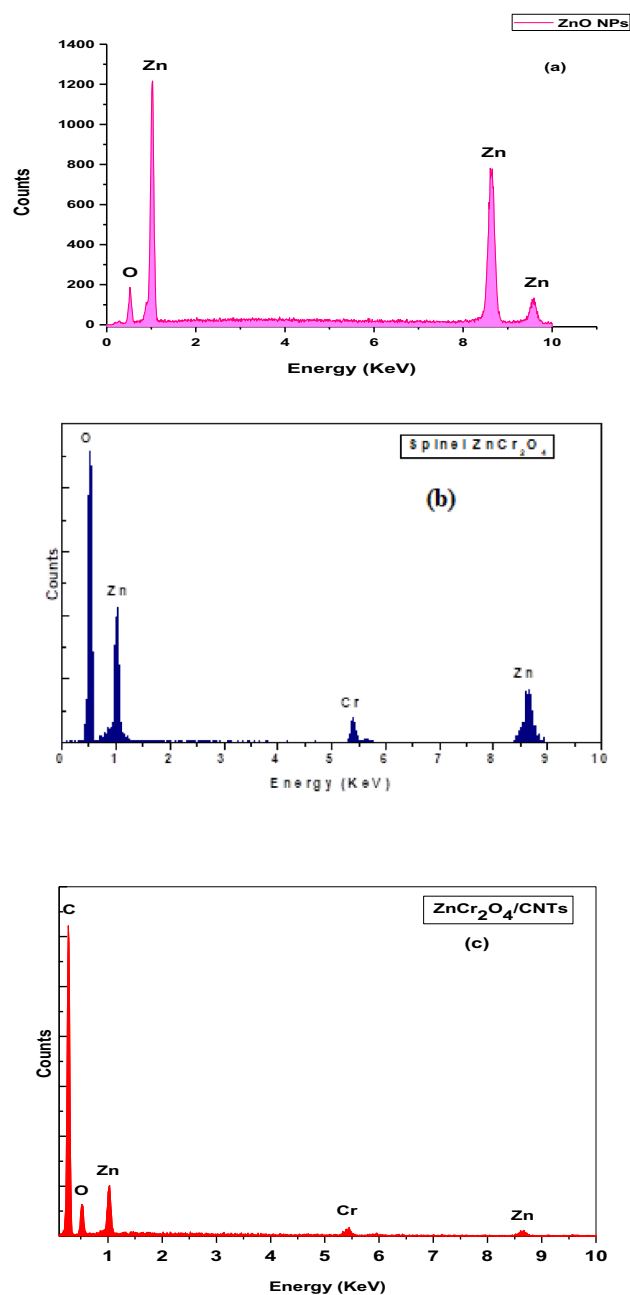
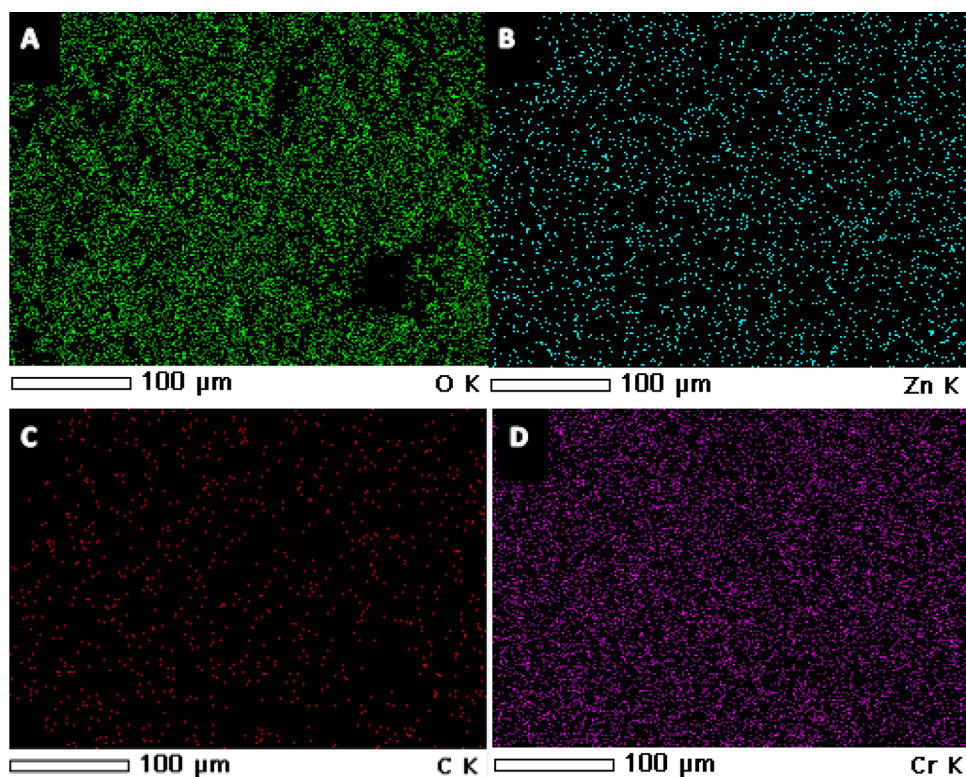


Fig. 2 EDX patterns of ZnO nanorods (a), ZnCr_2O_4 (b) and $\text{ZnCr}_2\text{O}_4/\text{MWCNTs}$ (c)

consistent with the XRD behavior. Figure 3A–D depicts the EDX color mapping of the elements Zn, O, C, and Cr which were homogeneously dispersed [44].

Figure 4a–c describes the TEM micrographs of the nanostructures. The TEM of ZnO shows the nanoparticles in spherical–hexagonal shape with mean size varied between 30 and 40 nm (Fig. 4a). Besides, the spinel ZnCr_2O_4 displayed a quasi-spherical particles of small diameter ~ 15 nm (Fig. 4b). Compared to ZnO, the particles of the spinel compound revealed a relative uniform distribution [45]. The

Fig. 3 EDX analysis of **A** Oxygen, **B** Zinc, **C** Carbon and **D** Chromium



TEM of the nanocomposite $\text{ZnCr}_2\text{O}_4/\text{MWCNTs}$ depicted spherical nanoparticles decorated with CNTs (Fig. 4c) [46]. Some of the nanoparticles were aggregated together due to the small particle size and large surface area. It is worthy to note that the obtained results from the TEM micrographs were consistent with the XRD behavior.

Electrochemical behavior of CLT at different sensors

Large surface area of the electrodes is a very important as it improves electrochemical activity and hence analytical performance. The electrodes active surface area can be determined by CV method consuming a solution of ($1 \times 10^{-3} \text{ mol L}^{-1}$) $\text{K}_4[\text{Fe}(\text{CN})_6]$ in 0.1 mol L^{-1} KCl for the reaction using Randles–Sevcik equation [47].

$$I_{pa} = (2.69 \times 10^5) n^{3/2} A_0 C_0 D_0^{1/2} v^{1/2}$$

The active surface area was estimated from the previous equation through the obtained slope. $\text{ZnCr}_2\text{O}_4/\text{MWCNT}/\text{CPE}$ shows irreversible oxidation reaction behavior toward CLT (Fig. 5). The response of $\text{ZnCr}_2\text{O}_4/\text{MWCNTs}$ was higher than the other modified electrodes ZnO/CPE , $\text{ZnCr}_2\text{O}_4/\text{CPE}$, and bare CPE. Modified electrode appears to increase electrochemical activity due to its large intrinsic surface area, and it enhances the transfer of electrons leading to the improvement of the electrochemical reaction. The active surface area of $\text{ZnCr}_2\text{O}_4/\text{MWCNTs}$ electrode was

0.291 compared to 0.199, 0.151, and 0.054 for ZnCr_2O_4 , ZnO , and bare CPE sensors, respectively. A solution contains ($6 \mu\text{mol L}^{-1}$) CLT was determined at a pH of 5 and a scan rate of 100 mV/s and the response of these four novel electrodes were compared; it was found that $\text{ZnCr}_2\text{O}_4/\text{MWCNTs}/\text{CPE}$ showed a greater response than other electrodes. $\text{ZnCr}_2\text{O}_4/\text{MWCNTs}/\text{CPE}$ shows significant enhancement in the peak current due to increase in the electroactive surface area and electrocatalytic activity (Figure 2S).

It was found that 9% $\text{ZnCr}_2\text{O}_4/\text{MWCNTs}$ NPs gave excellent response as verified by DPV (Figure 3S), while higher concentrations were found to be unsuitable owing to reduction of the electrode active area and block the electrode surface.

Optimization of the experimental conditions

Effect of pH

Phosphate buffer of pH range from 2 to 7 was tried to determine the suitable pH for $\text{ZnCr}_2\text{O}_4/\text{MWCNT}/\text{CPE}$ using the same CLT concentration ($6 \mu\text{mol L}^{-1}$). Shifting of the anodic peak occurred due to participation of electrons in the oxidation process as shown in Figure 4S (A). The protons to the electrons ratio was 1:1, and the reaction slope was 0.050, which was relatively close to the Nernstian hypothetical value (0.059). Consequently, pH had important effect on the reaction (Figure 4S) (B).

Fig. 4 TEM micrographs of **a** ZnO, **b** spinel ZnCr_2O_4 , and **c** $\text{ZnCr}_2\text{O}_4/\text{MWCNTs}$ nanocomposite

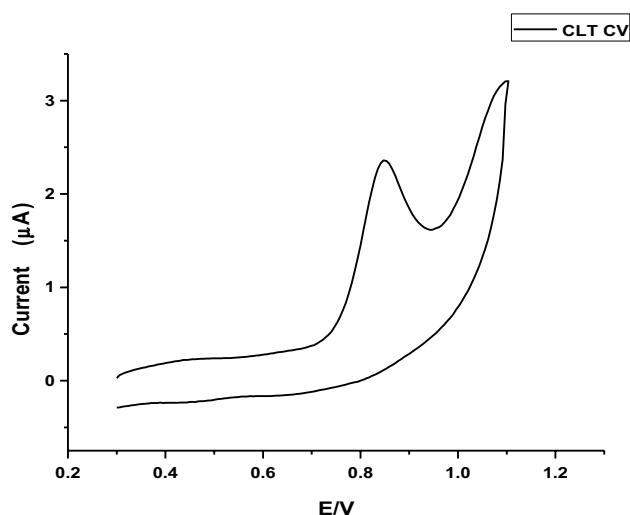
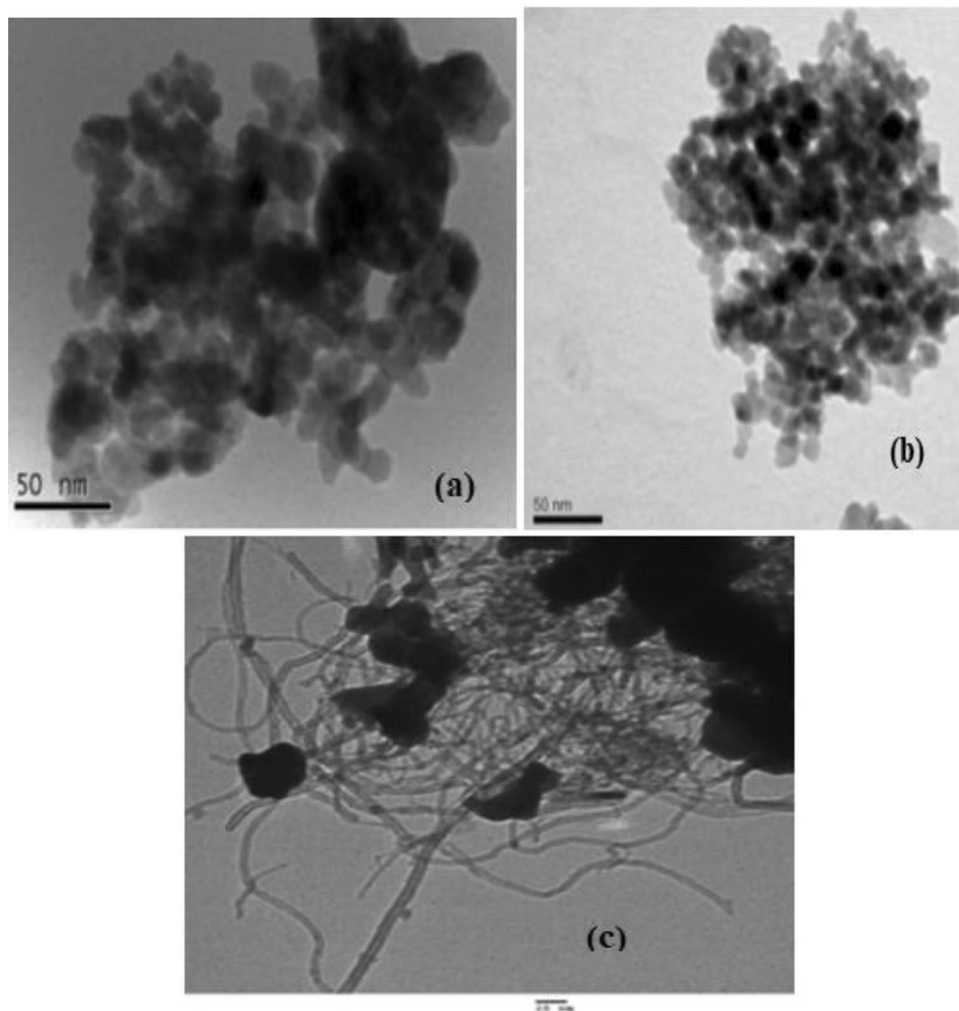


Fig. 5 CV of $\text{ZnCr}_2\text{O}_4/\text{MWCNTs}/\text{CPE}$ behavior for $1 \times 10^{-4} \text{ mol L}^{-1}$ CLT in PBS of pH 5 at scan rate of 100 mV/s

$$E_{pa} \text{ (V)} = -0.050 \text{ pH} + 1.096 \quad (5)$$

Scan rate optimization

Scan rate effect on the oxidation of CLT solution ($1 \times 10^{-4} \text{ mol L}^{-1}$) was investigated by measuring the response of the sensor using scan rates range from 20 to 140 mV/s (Figure 5S). The obtained results suggest that the oxidation behavior of CLT was due to mixed diffusion and adsorption mechanism on the $\text{ZnCr}_2\text{O}_4/\text{MWCNTs}$ electrode. Upon representing the log of peak current versus log of the scan rate, a linear relationship was obtained (Figure 5S) (inset B). The obtained slope was 0.797 which confirm mixed diffusion and adsorption mechanism for CLT oxidation.

$$\text{Log } I_p = 0.91 + 0.797 \text{ log } \nu \quad (6)$$

Diffusion of molecules from a great concentration to a small concentration was the principle of the mechanism of the electrode sensing. The electrons numbers contributing in

an electrochemical process can be determined using Laviron equation [48].

$$E = E^{\circ} + \left(\frac{2.303RT}{anF} \right) \log \left(\frac{RTK^{\circ}}{anF} \right) + \left(\frac{2.303RT}{anF} \right) \log v$$

Upon drawing log scan rate (log v) against potential (Figure 5S (Inset C)), αn can be calculated from the obtained slope, where n is the number of electrons transmitted and α is the electron transfer coefficient.

$$E_p(V) = 0.055 \log v + 0.899$$

The slope of the last equation is 0.055, and αn is 1.07. As CLT electro-oxidation process is irreversible, α was supposed to be 0.5 and n was determined to be ≈ 2 , which is in agreement with the suggested electro-oxidation mechanism shown in Scheme 1S.

Determination of CLT in pure form

Oxidation of CLT on ZnCr₂O₄/MWCNTs/CPE at applied potential range –0.2–1.4 V. CLT displayed an oxidation peak at 0.847 V by DPV. The method was found to be linear from 0.1–9 $\mu\text{mol L}^{-1}$, and the regression parameters are shown in Table 2.

Methods validation

Under the above-mentioned experimental conditions, the calibration graph was constructed as shown in Figure 6S and the linear regression parameters of CLT were determined and presented in Table 2.

Table 2 Regression parameters for CLT determination at ZnCr₂O₄/MWCNTs/CPE

Parameters	DPV method
Linearity ($\mu\text{mol L}^{-1}$)	0.1–9
Slope	0.039
Intercept	0.172
Accuracy ^a (%R)	99.45
Intermediate precision ^b (%RSD)	0.887
LOQ ($\mu\text{mol L}^{-1}$)	0.09
LOD ($\mu\text{mol L}^{-1}$)	0.03
Correlation coefficient (r)	0.9993
Repeatability (%RSD)	1.223
Robustness (%RSD)	1.801
Stability of the electrode (%RSD)	1.971

^a n Average of five determinations

^b n Average of three determinations

LOD and LOQ were determined using the following equations:

$$\text{LOD} = 3.3 \sigma / S$$

$$\text{LOQ} = 10 \sigma / S$$

where σ is the residual standard deviation of a regression line and S is the slope of the calibration curve. The values summarized in Table 2 demonstrate that the suggested method was sensitive for detection of low CLT concentrations.

Accuracy was assessed as % recovery of CLT concentrations and found to be near to the theoretical value. The values are summarized in Table 2.

Three different CLT concentrations were determined in the same day and in three successive days to estimate intra-day and interday precision of the fabricated ZnCr₂O₄/MWCNTs electrode. The precision as percent relative standard deviation (RSD %) was estimated (Table 2), and the technique appeared a worthy precision for CLT estimation.

Robustness refers to the capacity of an analytical method to be unaffected by slight changes without the occurrence of unexpected differences in the obtained results [49]. Upon small variation in a definite method parameters such as the response time ($10 \text{ s} \pm 0.3 \text{ s}$) and change of pH (5 ± 0.1), the response of CLT stayed relatively unchanged, confirming robustness of the procedure. The reusability was estimated by recording the response of a sensor used before and that of the recently synthesized sensor (more than ten times). Similar responses explain that the sensor can be reused. The reproducibility of the proposed electrode was determined by construction of six sensors under the optimum conditions, and %RSD was found to be 1.650, confirming that acceptable reproducibility. Within 30 days, sensor's stability was tested by recording the produced current. The peak current was remained up to 98% of its initial response through this period. As a result, the suggested sensor shows an excellent degree of reliability.

Application to dosage form

The developed procedure was useful for the quantification of CLT in tablets. The obtained results were in good consistency with the label claim, demonstrating that there is no interference from excipients and additives. DPV technique was applied to measure CLT successfully in tablets at ZnCr₂O₄/MWCNT/CPE electrode. The validity of the suggested method was further evaluated by the standard addition technique where acceptable results were attained (Table 3). By comparing the results obtained for determination of CLT in tablets with those of a published HPLC method [20], no important differences were found by applying t-test and F-test as shown in Table 4. The results obtained from ANOVA test (Table 1S) approve the accurate

Table 3 CLT determination by standard addition technique at ZnCr₂O₄/MWCNTs/CPE in commercial tablets

Tablets	Method	% Found \pm SD	Added ($\mu\text{mol L}^{-1}$)	Found ($\mu\text{mol L}^{-1}$)	% Recovery
Hygroton® labeled (50 mg/ tab)	DPV	99.56 \pm 0.34	0.2	0.199	99.50
			1.00	0.99	99.00
			3.00	3.02	100.67
			5.00	5.10	102.00
			7.00	6.93	99.00
			Mean \pm %RSD		100.03 \pm 1.156

Table 4 Statistical comparison of the developed method with the reported method for CLT estimation

Parameters	Developed method	HPLC reported method [20]
Mean	99.86	100.23
SD	1.110	0.925
Variance	1.232	0.855
<i>n</i>	5	5
Student's <i>t</i> -test	1.88 (2.306)*	–
<i>F</i> -test	1.44 (6.39)*	–

*The parenthesis contains the theoretical *F* and *t* values

Table 5 Validation parameters for the quantification of CLT in spiked human plasma and urine samples by DPV

Parameters	Plasma	Urine
Linearity ($\mu\text{mol L}^{-1}$)	0.3–9	0.3–9
Slope \pm SD ($\mu\text{mol L}^{-1}$)	0.04 \pm 0.004	0.039 \pm 0.005
Intercept \pm SD	0.103 \pm 0.054	0.111 \pm 0.034
Correlation coefficient (<i>r</i>)	0.998	0.997
Accuracy ^a (Mean \pm SD)	101.98 \pm 1.45	99.45 \pm 1.45
LOQ ($\mu\text{mol L}^{-1}$)	0.29	0.29
LOD ($\mu\text{mol L}^{-1}$)	0.095	0.093

^a*n* Average of five determinations

evaluation of CLT in the bulk and in tablet. Moreover, the developed procedure is more sensitive than the published procedures (Table 2S).

Application to spiked human plasma and urine

CLT was determined successfully in human plasma and urine. Oral administration of 25 mg per dose leads to absorption of above 75% of CLT to reach peak plasma concentration of about (192.2 ng/ml) after meal and (200.1 ng/ml) throughout fasting. The amount excreted unchanged in the urine was found to be about 27% of the dose [50]. The

published methods cannot be applied for determination of CLT in plasma because the c_{max} is out of their linearity, which suggest the need for the developed method. Remarkably, excellent results of CLT estimation in spiked plasma and urine were achieved; Table 5 confirms the ability of the developed method for the estimation of CLT without any interference in spiked plasma and urine samples.

Study of the electrode selectivity

The selectivity of the (ZnCr₂O₄/MWCNTs/CPE) to CLT was important parameter. The interference exhibited by materials found or introduced in the same dosage form with CLT was determined. Valsartan (VAL) as angiotensin receptor blockers has been widely used in combination with CLT (a potent diuretic). VAL was effective and safe to be administered with CLT in the same dosage form. The interference was determined by adding different VAL concentrations to fixed CLT concentration in phosphate buffer (pH 5.0), and the voltammetric current responses were recorded. It was observed that there was no significant variation in CLT oxidation peak current with increasing VAL concentrations and very small %RSD demonstrates that there is no significant interference confirming the high selectivity of the prepared electrode toward CLT (Figure 7S).

Assessment of the greenness of the proposed method

An important step nowadays in any established method is evaluating its greenness and impact on the environment. The Eco-scale assessment technique is depended on penalty points deducted from a base of 100. The novel constructed sensor was evaluated for its greenness by calculating penalty points, including instruments, reagents, and waste [51]. A high score indicates that the method is as smart green. It was found that the proposed method scored 83, as summarized in Table 3S, demonstrating that this novel fabricated electrode was considered as environmentally friendly.

Conclusion

The present work develops an electrochemical method based on modification of CPE by the incorporation of $\text{ZnCr}_2\text{O}_4/\text{MWCNTs}$ to determine CLT in pure, dosage form, and biological fluids. $\text{ZnCr}_2\text{O}_4/\text{MWCNTs}/\text{CPEs}$ electrode was found to enhance electrical conductivity more than unmodified CPE electrode. The developed method can effectively determine CLT with low detection limit, high sensitivity, selectivity, good reproducibility, and repeatability; it extended for determination of CLT in plasma and urine.

Supplementary Information The online version contains supplementary material available at <https://doi.org/10.1007/s13738-023-02843-5>.

Author contributions AMA-R designed the experiments and performed writing and editing. MMF performed supervision, examined and interpreted the data, and performed writing and editing. NSR performed supervision, examined and interpreted the data, and performed writing and editing. AIH performed the experiments, contributed reagents and materials, wrote the paper, and provided analysis tools or data. EE investigated the data and performed writing and editing.

Funding The authors didn't obtain any funding from any organization.

Availability of data and materials Most of data analyzed during this work were included in this published article and those not involved are available from the corresponding author on reasonable request.

Declarations

Conflict of interest All authors state that there is no conflict of interest regarding the publication of this work.

References

1. A. Vasilescu, A. Hayat, S. Gáspár, J.L. Marty, Advantages of carbon nanomaterials in electrochemical aptasensors for food analysis. *Electroanalysis* **30**(1), 2–19 (2018)
2. I.M. Mostafa, C. Meng, Z. Dong, B. Lou, G. Xu, Potentiometric sensors for the determination of pharmaceutical drugs. *Anal. Sci.* **38**(1), 23–37 (2022)
3. A.M. Abdel-Raouf, M.M. Fouad, N.S. Rashed, N.Y.Z. Hosni, A. Elsonbaty, A. Abdel-Fattah, Potentiometric determination of mebeverine hydrochloride antispasmodic drug based on molecular docking with different ionophores host-guest inclusion as a theoretical study. *RSC Adv.* **13**(2), 1085–1093 (2023)
4. A.M. Abdel-Raouf, A. Elsonbaty, S. Abdulwahab, W.S. Hassan, M.S. Eissa, Potentiometric determination of amprolium drug at a carbon nanotubes/nickel oxide nanoparticles paste electrode. *Microchem. J.* **165**, 106185–106192 (2021)
5. A. Elsonbaty, K. Attala, Application of experimental design approaches and in silico molecular docking on the host-guest complexes with cyclodextrin for the analysis of benazepril hydrochloride in pharmaceutical formulation. *J. Electrochem. Soc.* **168**(5), 057515 (2021)
6. S.A. Hassan, N.W. Nashat, M.R. Elghobashy, S.S. Abbas, A.A. Moustafa, A.M. Mahmoud, Novel microfabricated solid-contact potentiometric sensors doped with multiwall carbon-nanotubes for simultaneous determination of bisoprolol and perindopril in spiked human plasma. *Microchem. J.* **178**, 107323–107331 (2022)
7. S. Jeong, J. Park, D. Pathania, C.M. Castro, R. Weissleder, H. Lee, Integrated magneto–electrochemical sensor for exosome analysis. *ACS Nano* **10**(2), 1802–1809 (2016)
8. F. Cui, Z. Zhou, H.S. Zhou, Measurement and analysis of cancer biomarkers based on electrochemical biosensors. *J. Electrochem. Soc.* **167**(3), 037525 (2019)
9. B. Bozal-Palabiyik, C. Erkmen, S. Kurbanoglu, S.A. Ozkan, B. Uslu, Electrochemical analysis for pharmaceuticals by the advantages of metal oxide nanomaterials. *Curr. Anal. Chem.* **17**(9), 1322–1339 (2021)
10. C.M. Welch, R.G. Compton, The use of nanoparticles in electroanalysis: a review. *Anal. Bioanal. Chem.* **384**(3), 601–619 (2006)
11. H. Song, D. Laudenschleger, J.J. Carey, H. Ruland, M. Nolan, M. Muhler, Spinel-structured ZnCr_2O_4 with excess Zn is the active $\text{ZnO}/\text{Cr}_2\text{O}_3$ catalyst for high-temperature methanol synthesis. *ACS Catal.* **7**(11), 7610–7622 (2017)
12. R. Mimouni, O. Kamoun, A. Yumak, A. Mhamdi, K. Boubaker, P. Petkova, M. Amlouk, Effect of Mn content on structural, optical, opto-thermal and electrical properties of ZnO: Mn sprayed thin films compounds. *J. Alloys Compd.* **645**, 100–111 (2015)
13. United States Pharmacopeia, 30th Ed. Rockville, MD: The US Pharmacopeial Convention; 2006
14. W. Martindale, K. Parfitt, Martindale: The Complete Drug Reference. Pharmaceutical Press London (2009)
15. N.S. Abdullah, M.A. Hassan, R.O. Hassan, Spectrophotometric determination of chlorthalidone in pharmaceutical formulations using different order derivative methods. *Arab. J. Chem.* **10**, S3426–S3433 (2017)
16. K. Attala, A. Elsonbaty, Advanced eco-friendly UV spectrophotometric approach for resolving overlapped spectral signals of antihypertensive agents in their binary and tertiary pharmaceutical dosage form. *Spectrochim. Acta A Mol. Biomol. Spectrosc.* **258**(5), 119855–119864 (2021)
17. S.R. Chaudhari, A.A. Shirkhedkar, Exploration of 1, 2-naphthoquinone-4-sulfonate derivatizing reagent for determination of chlorthalidone in tablets: a spectrophotometric investigation. *Future J. Pharm. Sci.* **7**(1), 1–9 (2021)
18. W.M. Ebeid, E.F. Elkady, A.A. El-Zaher, R.I. El-Bagary, G. Patonay, Spectrophotometric and spectrofluorimetric studies on azilsartan medoxomil and chlorthalidone to be utilized in their determination in pharmaceuticals. *Anal. Chem. Insights* **9**(9), 33–40 (2014)
19. A. Elsonbaty, M.A. Hasan, M.S. Eissa, W.S. Hassan, S. Abdulwahab, Synchronous spectrofluorimetry coupled with third-order derivative signal processing for the simultaneous quantitation of telmisartan and chlorthalidone drug combination in human plasma. *J. Fluoresc.* **31**(1), 97–106 (2021)
20. C. Kharat, V.A. Shirsat, Y.M. Kodgule, M. Kodgule, Validated RP-HPLC stability method for the estimation of chlorthalidone and its process-related impurities in an API and tablet formulation. *Int. J. Anal. Chem.* **2020**(7), 1–11 (2020)
21. A.A. Elshanawane, S.M. Mostafa, M.S. Elgawish, Development and validation of a reversed-phase high-performance liquid chromatographic method for the simultaneous determination of amiloride hydrochloride, atenolol, hydrochlorothiazide, and chlorthalidone in their combined mixtures. *J. AOAC Int.* **92**(2), 404–409 (2009)
22. K. Jagadeesh, N. Annapurna, Stability indicating method to analyze benidipine and chlorthalidone using HPLC technique: Establishment, validation and application to tablets. *Pharm. Sci.* **26**(1), 75–81 (2020)
23. M.S. Elgawish, S.M. Mostafa, A.A. Elshanawane, Simple and rapid HPLC method for simultaneous determination of atenolol

- and chlorthalidone in spiked human plasma. *Saudi. Pharm. J.* **19**(1), 43–49 (2011)
24. W.M. Ebeid, E.F. Elkady, A.A. El-Zaher, R.I. El-Bagary, G. Patonay, Stability-indicating RP-LC method for determination of azilsartan medoxomil and chlorthalidone in pharmaceutical dosage forms: application to degradation kinetics. *Anal. Bioanal. Chem.* **406**(26), 6701–6712 (2014)
 25. A. El-Gindy, S. Emar, A. Mostafa, HPLC and chemometric-assisted spectrophotometric methods for simultaneous determination of atenolol, amiloride hydrochloride and chlorthalidone. *Farmaco* **60**(3), 269–278 (2005)
 26. N.S. Abdelwahab, Determination of atenolol, chlorthalidone and their degradation products by TLC-densitometric and chemometric methods with application of model updating. *Anal. Methods* **2**(12), 1994–2001 (2010)
 27. A.J. Vyas, D.A. Gol, R.G. Usdad, A.I. Patel, A.B. Patel, N.K. Patel, A. Chudasama, HPTLC-densitometric method for simultaneous estimation of olmesartan medoxomil and chlorthalidone in tablet dosage form. *Anal. Chem. Lett.* **10**(4), 498–506 (2020)
 28. K. Al Azzam, A. A. Elbashir, M. A. Elbashir, B. Saad, S. Abdul Hamid, Simultaneous determination of atenolol and chlorthalidone in pharmaceutical preparations by capillary-zone electrophoresis. *Anal. Lett.* **42**(10), 1458–1470 (2009)
 29. A. Khuroo, S. Mishra, O. Singh, S. Saxena, T. Monif, Simultaneous determination of atenolol and chlorthalidone by LC–MS–MS in human plasma. *Chromatographia* **68**(9), 721–729 (2008)
 30. O. Gonzalez, G. Iriarte, E. Rico, N. Ferreirós, M.I. Maguregui, R.M. Alonso, R.M. Jiménez, LC–MS/MS method for the determination of several drugs used in combined cardiovascular therapy in human plasma. *J. Chromatogr. B* **878**(28), 2685–2692 (2010)
 31. T. Choezom, B. Gurupadaya, Validated chiral RP-UFLC method for the quantification of chlorthalidone in bulk and pharmaceutical dosage form. *Int. J. Appl. Pharm.* **9**(2), 22–27 (2017)
 32. J. Vozka, K. Kalíková, E. Tesařová, Rapid supercritical fluid chromatography method for separation of chlorthalidone enantiomers. *Anal. Lett.* **46**(18), 2860–2869 (2013)
 33. K.A.M. Attia, A.H. Abdel-Monem, A.M. Ashmawy, A.S. Eissa, A.M. Abdel-Raouf, Construction and application of highly sensitive spinel nanocrystalline zinc chromite decorated multiwalled carbon nanotube modified carbon paste electrode (ZnCr_2O_4 @MWCNTs/CPE) for electrochemical determination of alogliptin benzoate in bulk and its dosage form: green chemistry assessment. *RSC Adv.* **12**(33), 19133–19143 (2022)
 34. M. Chinnasamy, K. Balasubramanian, Enhanced UV photodetection behavior of Cr doped wurtzite ZnO crystalline nanorods. *Opt. Mater.* **110**, 110492–110500 (2020)
 35. G.N. Rajivgandhi, G. Ramachandran, N.S. Alharbi, S. Kadai-kunnan, J.M. Khaleed, N. Manokaran, W.J. Li, Substantial effect of Cr doping on the antimicrobial activity of ZnO nanoparticles prepared by ultrasonication process. *Mater. Sci. Eng. B.* **263**, 114817–114824 (2021)
 36. H. Tajizadegan, A. Heidary, O. Torabi, M.H. Golabgir, A. Jamshidi, Synthesis and characterization of ZnCr_2O_4 nanospinel prepared via homogeneous precipitation using urea hydrolysis. *Int. J. Appl. Ceram. Technol.* **13**(2), 289–294 (2016)
 37. G. Thennarasu, A. Sivasamy, Synthesis and characterization of nanolayered $\text{ZnO}/\text{ZnCr}_2\text{O}_4$ metal oxide composites and its photocatalytic activity under visible light irradiation. *J. Chem. Technol. Biotechnol.* **90**(3), 514–524 (2015)
 38. S.K. Sharma, R. Gupta, G. Sharma, K. Vemula, A.R. Koirala, N.K. Kaushik, E.H. Choi, D.Y. Kim, L.P. Purohit, B.P. Singh, Photocatalytic performance of yttrium-doped CNT-ZnO nano-flowers synthesized from hydrothermal method. *Mater. Today Chem.* **20**, 100452–100461 (2021)
 39. J.M. Yusof, I. Ismail, M.R. Yusop, S.A. Rashid, Morphological effect on conductivity performance of ZnO/carbon nanotubes cotton hybrid. *Appl. Surf. Sci. Adv.* **7**, 100211–100217 (2022)
 40. R. Zamiri, B. Singh, M.S. Belsley, J. Ferreira, Structural and dielectric properties of Al-doped ZnO nanostructures. *Ceram. Int.* **40**(4), 6031–6036 (2014)
 41. A. Sharma, R.K. Khangarot, K.P. Misra, R.D.K. Misra, S. Chattopadhyay, P.D. Babu, N. Halder, Band gap reduction and quenching of p-d exchange interaction in sol-gel derived Zn(Al,Cu)O nanostructures. *Phys. Scr.* **96**(7), 075803 (2021)
 42. P.K. Pandey, V. Chauhan, P. Dixit, P.C. Pandey, Correlation of enhanced photocurrent with structural and optical properties of Ag–ZnO nanocomposites synthesized by a facile chemical route. *Phys. B Condens. Matter.* **612**, 412937–412944 (2021)
 43. K. Tantubay, P. Das, Hydrogen peroxide-assisted photocatalytic dye degradation over reduced graphene oxide integrated ZnCr_2O_4 nanoparticles. *Environ. Sci. Pollut. Res.* **29**(12), 17309–17318 (2022)
 44. D. Wang, J. Guo, C. Cui, J. Ma, A. Cao, Controllable synthesis of CNT@ZnO composites with enhanced electrochemical properties for lithium-ion battery. *Mater. Res. Bull.* **101**, 305–310 (2018)
 45. A.A. Ismail, S.M. Albukhari, M. Mahmoud, Mesoporous ZnCr_2O_4 photocatalyst with highly distributed PtO nanoparticles for visible-light-induced photoreduction of nitrobenzene. *Opt. Mater.* **122**, 111676 (2021)
 46. Z. Shahnava, S.B. Abd Hamid, Fabrication of a novel metal chromite–Carbon nanotube composite for the highly efficient electrocatalytic reduction of hydrogen peroxide. *Appl. Surf. Sci.* **407**, 379–385 (2017)
 47. A.M. Abdel-Raouf, M.A. El-Shal, R.A. Said, M.H. Abostate, S. Morschedy, M.S. Emar, Versatile sensor modified with gold nanoparticles carbon paste electrode for anodic stripping determination of brexpiprazole: a voltammetric study. *J. Electrochem. Soc.* **166**(12), B948–B955 (2019)
 48. A.J. Bard, L.R. Faulkner, Basic potential step methods. *Electrochem. Methods Fundam. Appl.* 156–225 (2001)
 49. Y. Vander Heyden, A. Nijhuis, J. Smeyers-Verbeke, B. Vandeginste, D. Massart, Guidance for robustness/ruggedness tests in method validation. *J. Pharm. Biomed. Anal.* **24**(5–6), 723–753 (2001)
 50. C. Dudkowski, A. Karim, M. Munsaka, Effects of food intake on the pharmacokinetics of azilsartan medoxomil and chlorthalidone alone and in fixed-dose combination in healthy adults. *Clin. Pharmacol. Drug Dev.* **5**(5), 393–398 (2016)
 51. M. Tobiszewski, Metrics for green analytical chemistry. *Anal. Methods* **8**(15), 2993–2999 (2016)

Springer Nature or its licensor (e.g. a society or other partner) holds exclusive rights to this article under a publishing agreement with the author(s) or other rightsholder(s); author self-archiving of the accepted manuscript version of this article is solely governed by the terms of such publishing agreement and applicable law.